EQUIVALENT CIRCUIT APPROACH TO THE RADOME PROBLEM

I. LOADED DIELECTRICS

by

B. A. LIPPMANN and A. OPPENHEIM

April 30, 1954

CONTRACT Nonr 1233(00)
OFFICE OF NAVAL RESEARCH

TECHNICAL RESEARCH GROUP
56 West 45th Street
New York 36, New York

LOADED DIELECTRICS

by

B. A. LIPPMANN and A. OPPENHEIM

April 30, 1954

This is the first of three reports bearing the general title "Equivalent Circuit Approach to the Radome Problem". Each of the reports may be read independently of the others.

CONTRACT Nonr 1230(00)
OFFICE OF NAVAL RESEARCH

TECHNICAL RESEARCH GROUP
56 West 45th Street
New York 36, New York

ABSTRACT

Equivalent circuit techniques are used to analyze the scattering properties of several different loaded dielectrics. These include: parallel plates, dielectric slabs loaded internally, and dielectric slabs loaded on both sides by wire screens. In the appendix, some remarks are made concerning the problem of inductive or capacitive obstacles exposed to free space on one side and a dielectric on the other.

ACKNOWLEDGMENT:

We are very much indebted to Professor N. Marcuvitz for consultative assistance in connection with this work.

EQUIVALENT CIRCUIT APPROACH TO THE RADOME PROBLEM

I. Loaded Dielectrics

1. Introduction

2. General Remarks

   2a. E- and H-mode transmission lines

   2b. Loaded dielectrics

   2c. "Simple loading"

   2d. "Complex loading"

   2e. "Uniform loading"

3. Numerical Analyses

   3a. H-mode parallel plates (semi-infinite)

   3b. H-mode dielectric (semi-infinite)

   3c. E-mode dielectric (semi-infinite)

   3d. H-mode dielectric slab

   3e. Wire screens

   3f. Dissipation

   3g. H-mode plates: Junction effects

4. Appendices

   4a. Transmission and reflection formulas

   4b. Impedance and propagation constant of a loaded line

   4c. Interface impedances

EQUIVALENT CIRCUIT APPROACH TO THE RADOME PROBLEM

I

LOADED DIELECTRICS

1. Introduction

The Princeton Report[1] treated the design of a radome material from the viewpoint of molecular optics. Here, the problem is approached from the standpoint of "equivalent circuits".

The use of equivalent circuit techniques could be discussed in terms of abstract theory. We prefer, however, to illustrate the method involved by detailed numerical analyses of specific examples. The particular structures chosen for analysis have been suggested by the investigations of H. R. Worthington[2], to whom we are indebted for advance accounts of his work, both by correspondence and personal discussion.

Worthington has been led to consider structures, of the type analyzed here, by an ingenious series of theoretical and experimental studies. His work forms a useful starting point for the present, purely theoretical, discussion, not only because of the intrinsic interest of the results, but also because of his use of equivalent circuit concepts.

Accordingly, this report is partly a commentary on, and partly a supplement to, Worthington's work; in some respects it is an extension, in others it is an alternative, occasionally more rigorous, formulation of his analysis.

The plan of this report is as follows: We start with some generalities on the problem of matching a dielectric to free space (Sec. 2); these remarks are deliberately brief. The major portion of the report is devoted to the numerical analysis of a few particular loaded dielectrics (Sec. 3). In the course of illustrating our approach by means of these special examples, some general questions are encountered. The discussion of these matters is reserved for the Appendices (Sec. 4).

2. General Remarks

2a. E- and H-mode transmission lines: Suppose a plane wave is incident on a dielectric from free space (Fig. 1a). As is customary, we distinguish between the two polarizations: E-vector (a) parallel, and (b) perpendicular, to the plane of incidence. However, using the language[3] of the modal analysis, we shall call (a) an E-wave (or mode), and (b) an H-wave.

A modal analysis is useful whenever, as in Fig. 1a, a direction exists (direction of transmission) such that the determination of the field variations transverse to this direction is trivial. The transverse variations may then be

suppressed, leaving a one-dimensional problem involving only the direction of transmission. With respect to this direction, the field variations corresponding to each mode are of the transmission line type.

The quantities[4] that are required to describe each mode as a transmission line of the E- or H-type are summarized in Fig. 1. We note that:

i) The E- and H-mode transmission lines are duals of each other. This makes it simple to transform, by duality, from the case where ε alone varies to the case where μ alone varies. In the remainder of this report, we shall assume that only ε varies as we change media.

ii) The relations in Fig. 1a are independent of polarization. As a consequence, the phase shifts for E- and H-waves are the same in homogeneous media.

iii) If both regions are uniform in the transverse direction, as in Fig. 1a, Snell's Law holds (k_c same in both regions).

2b. Loaded dielectrics: Let $\varepsilon_2 = \varepsilon_1 + \delta\varepsilon$ in Fig. 1a. One approach to the radome problem asks: Can we, by loading medium 2 with suitable obstacles, eliminate the influence of $\delta\varepsilon$, so that the gross properties of the composite medium--characteristic impedance and propagation constant--are identical

to those of medium 1? In discussing this question, we shall arbitrarily divide the types of loading into three classes:

"Simple loading". The obstacles used have a geometrical structure sufficiently simple to enable the field problem they present to be solved using a single mode.

"Complex loading". More than one mode is required to solve the field problem.

"Uniform loading". The obstacle spacing is so close ($\ll\lambda$) that the new medium may be regarded as homogeneous.

2c. "Simple loading". We ask: (a) If an E- (or H-) mode is incident from region 1, can we arrange a set of obstacles in region 2 so that only a single E- (or H-) mode can propagate in region 2? (b) If so, can we further arrange the obstacle spacings so that $Z_1 = Z_2$ and $\kappa_1 = \kappa_2$?

Regarding (a), we note that one type of obstacle that could be used to provide "simple loading" is a set of parallel plates; this kind of loading, applied to the H-mode case, is analyzed numerically in Section 3a.

Turning to (b): From the relations in Fig. 1, since ω and μ are the same in both media, we see that, in the H-mode case, if

(2c-1) $$Z_1 = Z_2$$

then we will simultaneously have

(2c-2) $$K_1 = K_2$$

In the E-mode case, however, the imposition of (2c-1) implies

(2c-3) $$\frac{K_1}{\epsilon_1} = \frac{K_2}{\epsilon_2}$$

Thus, for H-modes, a set of obstacles that makes $Z_1 = Z_2$ at the same time results in $K_1 = K_2$; in the E-mode case, if $Z_1 = Z_2$, we cannot have, concurrently, $K_1 = K_2$.

Further, we note that K_1 is a function of θ_1. "Simple loading", by definition, corresponds to a single mode in region 2; i.e., a single value of K_2. It follows that a given set of "simple" obstacles can satisfy (2c-1) at only one value of θ_1.

A physical interpretation of these remarks can be based on Figs. 1b, c, and an analysis of the extent to which changes of k_c in these figures can be used to compensate changes in ϵ.

2d. "Complex loading" : In this category, we limit the discussion to the following: The "elementary scatterer" is a thin obstacle that scatters more than one mode; such scatterers are located at periodic intervals in the transverse plane to form

a two-dimensional lattice. Several such arrays may be arranged in successive layers along the direction of transmission.

The lattice periods, in the transverse planes, are assumed to be less than $\lambda/2$; i.e., only a single "propagating" mode exists. In the longitudinal direction, successive layers are separated sufficiently to insure that they inter-act only through the single "propagating" mode.

With the imposition of these conditions, the unloaded medium may be represented by a transmission line and the loading by shunt elements on the line, one to represent each array.

This type of loading is analyzed in Secs. 3e, 3F. The methods used are also applicable to any other arrays that satisfy the requirements stated above.

2e. "Uniform loading": According to iii) of Sec. 2a, if the loading is uniform in region 2, $k_{c_1} = k_{c_2}$ at all angles of incidence. It then follows that all the inductances in Figs. 1b, c are unchanged as we go from one medium to the other, while the capacitances increase as we go from 1 to 2. For E-modes, this changes both the series impedance and the shunt admittance of the equivalent transmission line; for H-modes, only the shunt admittance is changed. To eliminate these changes by uniform loading, the E-modes require obstacles that present a series capacitance and a shunt inductance; the H-modes require obstacles that can be represented by a shunt inductance.

Now, an analysis of the field problem shows, in general, that a thin obstacle, when regarded from the proper reference plane, usually has a purely shunt element as its equivalent circuit, while a thick obstacle requires both series and shunt elements to represent it.

Thus, insofar as the effect of $\delta\varepsilon$ in medium 2 can be compensated for at all by uniform loading, we conclude that:

(a) H-modes require that medium 2 be loaded with thin obstacles.

(b) E-modes require loading with thick obstacles.

(c) Both modes require inductive shunt elements; in addition, the E-modes also require capacitative series elements.

It follows that, when ε increases, the compensation of an H-mode should be easier than that of an E-mode. What is required, for the H-mode, is a fairly dense distribution of thin, conducting obstacles shaped so that no charges accumulate on their surfaces. A regular array of such elements is not necessary; a statistical distribution will do.

For example, a simple shunt obstacle that is purely inductive, for H-modes, is a thin, infinitely long wire parallel to the electric field. Wires of finite length may also be used if they are inductive at the operating frequency (i.e., are resonant below the operating frequency, as remarked in the

Princeton Report[1]). The lengths of the wires are fixed by the inductance required. Their thicknesses can be determined by the bandwidth desired, for the Q of the wire will be proportional to the ratio of volume to surface of the region external to the wire.

Although these considerations could be made quantitative, this will not be done here. "Uniform loading" may be regarded as the limit of "complex loading" as the obstacle separation decreases. In the limit, separation $<< \lambda$, but large enough so that only the dominant mode interacts, the equivalent circuit analysis reduces to the molecular optics analysis.

3. Numerical Analyses

3a. H-mode parallel plates (semi-infinite): The geometry is shown in Fig. 2a. On the left is a homogeneous medium ($\varepsilon_1 = 1$). On the right is a set of semi-infinite conducting plates, of zero thickness, aligned parallel to the electric field and embedded in a medium of dielectric constant $\varepsilon_2 = \varepsilon$. Each region, 1 or 2, alone can be represented by an appropriate transmission line; only the junction effect requires special consideration.

The junction effect is described by three parameters (dissipationless quadripole). These may be taken to be two reference planes (T_1 and T_1' in Figs. 2a, b) and an ideal transformer[5] (symbolized in Fig. 2b by its turns ratio n). In Fig. 2b, the right hand end of line 1 is located on reference plane T_1; the left hand end of line 2 is on the reference plane T_1'.

If $\varepsilon_1 = \varepsilon_2$, it is known[6] that, for proper choice of T_1 and T_1', $n^2 = 1$. If there is no junction effect at all, as in Fig. 1a, we not only have $n^2 = 1$, but also $d = d' = 0$.

In general, d and d' will vary with the angle of incidence, θ_1. However, d and d' are required only if the phase of the reflected, or transmitted, wave is desired--or if the plates are of finite length. If we calculate the power reflected from, or transmitted into, the semi-infinite plates of Fig. 2a, d and d' are not needed.

We shall take advantage of this. By calculating power only, we shall eliminate the reference planes from the calculation; only the value of n^2 will be necessary. Taking $n^2 = 1$ will then be equivalent to ignoring the junction effect completely.

In this Section, mostly for didactic purposes, we shall take $n^2 = 1$; the more accurate calculation, including the junction effect, is given in Sec. 3g. We shall see that the junction effect is important.

Returning to Fig. 2a, we note that the separation of the plates is not arbitrary. "a" is bounded from above and below by the requirements that only the lowest modes propagate in regions 1 and 2.

(3a-1) $a < \frac{\lambda_1}{\sqrt{\varepsilon}} < 2a < \lambda_1$

To fix a convenient value for "a", we use the connection with K_2:

(3a-2) $$K_2 = \sqrt{k_2^2 - k_{c_2}^2} = \sqrt{k_1^2 \varepsilon - (\pi/a)^2}$$

Here, K_2 may be fixed by the requirement that $Z_2 = Z_1$ (and therefore $K_2 = K_1$) at some value of θ_1, say $\theta_1 = \theta_o$:

(3a-3) $$K_2 = k_1 \cos \theta_o$$

From Fig. 2b, therefore,

(3a-4) $$Z_2/Z_1 = \cos \theta_1 / \cos \theta_o$$

For unit incident power, the transmitted power, P_t, is, according to (4a-5):

(3a-5) $$P_t = 1 - \left(\frac{\cos \theta_1 - \cos \theta_o}{\cos \theta_1 + \cos \theta_o} \right)^2$$

Curves of P_t vs. θ_1, for $\theta_o = 0^\circ$, 50°, and 60° are plotted in Fig. 3. A discussion is given in the next section.

3b. H-mode dielectric (semi-infinite): For comparison with the parallel plates of the previous section, we have computed the transmission of an H-mode from free space into a semi-infinite dielectric ($\varepsilon = 2.59$). The result is plotted in Fig. 3.

The geometry is the same as Fig. 1a with $\varepsilon_1 = 1$ and $\varepsilon_2 = 2.59$. The equivalent circuit of Fig. 2b applies here if

we set $d = d' = 0$ and $n^2 = 1$. Z_2/Z_1 is given by:

$$(3b\text{-}1) \qquad \frac{Z_2}{Z_1} = \frac{K_1}{K_2} \cdot \frac{\cos\theta_1}{\sqrt{\epsilon - 1 - \cos^2\theta_1}}$$

As before, P_t is computed by putting this value of Z_2/Z_1 in (4a-5).

In the limit $\epsilon \gg 1$,

$$(3b\text{-}2) \qquad P_t \sim \frac{4}{\sqrt{\epsilon}} \cdot \cos\theta_1$$

Turning now to Fig. 3, and taking the range of incident angles for which $P_t > 90\%$ as an arbitrary figure of merit, we see that, insofar as the junction effect may be ignored, "simple loading" would seem to be useful. The bare dielectric falls below 90% transmission when $\theta_1 > 40^\circ$. "Simple loading", matched at $\theta_o = 0^\circ$, has $P_t = 1$ at normal incidence and P_t falls below 90° only for $\theta_1 > 60^\circ$. Matching at $\theta_o = 50^\circ$, or $\theta_o = 60^\circ$ causes the performance to deteriorate at small angles of incidence, but extends the 90% point to 70° and 75° respectively.

Moving the matching angle, θ_o, to large angles, in order to improve the performance at large angles, always reduces the transmission at small incident angles. For, since (3a-5) is symmetrical in θ_o and θ_1, the value corresponding to $\theta_o = \alpha$, $\theta_1 = 0$, is the same as that for $\theta_o = 0$, $\theta_1 = \alpha$. As a result, the $\theta_o = 0$ curve can be used to give the deterioration at low angles. For example, since the $\theta_o = 0$ curve passes through $P_t = .9$ at $\theta_1 = 60^\circ$, the $\theta_o = 60^\circ$ curve shows the best that can be done

at high angles if the low angles transmission is not to fall below 90%.

Since they are based on the results of Sec. 3a, these remarks are, of course, only approximately true, for the junction effect was ignored in Sec. 3a. The modifications introduced by the junction effect are given in Sec. 3g.

We remark that these results, although for semi-infinite media, also having a meaning for slabs of finite thickness. This arises because we are looking for very high transmissions, so high that two or more reflections may become negligible. If the successive reflections within the slab may be ignored, the slab may be treated using the simpler calculation applicable to a semi-infinite medium.

3c. E-mode dielectric (semi-infinite): The H-mode parallel plates described in Section 3a have transmission curves that closely resemble those obtained when an E-mode is incident on a dielectric. For an E-mode incident in Fig. 1a, ($\epsilon_1 = 1$: $\epsilon_2 = \epsilon$), the equivalent circuit is again given by Fig. 2b ($d = d' = 0$; $n^2 = 1$) except that now:

(3c-1) $$\frac{Y_2}{Y_1} = \frac{\epsilon_2 K_1}{\epsilon_1 K_2} = \frac{\epsilon \cos \theta_1}{\sqrt{\epsilon - 1 + \cos^2 \theta_1}}$$

The dielectric is matched to free space at the Brewster angle θ_B, where

(3c-2) $$\tan \theta_B = \sqrt{\epsilon}$$

Using this, (3c-1) can be rewritten as:

$$\frac{Y_2}{Y_1} = \frac{\mathcal{E} \cos \theta_1}{\sqrt{(\mathcal{E}^2 - 1) \cos^2 \theta_B + \cos^2 \theta_1}}$$

Or,

$$\text{(3c-3)} \qquad \frac{Y_2}{Y_1} \sim \frac{\cos \theta_1}{\cos \theta_B} \quad ; \text{ if } \sqrt{\mathcal{E}} >> 1$$

From (4a-5), therefore, for unit incident power,

$$\text{(3c-4)} \qquad P_t = 1 - \left(\frac{\cos \theta_1 - \cos \theta_B}{\cos \theta_1 + \cos \theta_B} \right)^2$$

Comparing (3c-4) and (3a-5), we see that the E-mode power transmitted by a dielectric is similar to the H-mode power transmitted (ignoring the junction effect)* through a set of parallel plates. The correspondence between θ_B and θ_o implies only that the "angle of match" must be the same in both cases. Of course, the condition $\sqrt{\mathcal{E}} >> 1$ is assumed to hold.

In Fig. 4, $\mathcal{E}$ has been taken as 2.59 (plexiglass) and P_t plotted using the exact relation (3c-1) and the approximation (3c-3). Even for this small value of $\mathcal{E}$, the error in using (3c-4) is less than 4%.

---

* The junction effect does not change this qualitative remark, since it can only introduce a transformer ratio into (3c-4).

3d. H-mode dielectric slab: In Fig. 5a, a dielectric slab, dielectric constant ε, is bounded on both sides by free space. The equivalent circuit is shown in Fig. 5b. The reference planes T_1, T_1' coincide with the two faces of the slab.

According to (4a-10), the power transmission $|T|^2$ is:

$$(3d\text{-}1) \qquad |T|^2 = \left[1 + \left(\frac{\frac{Z_2}{Z_1} - \frac{Z_1}{Z_2}}{2}\right)^2 \sin^2 K_2 \ell\right]^{-1}$$

For an H-mode incident, Z_2/Z_1 is given by (3b-1), while

$$(3d\text{-}2) \qquad K_2 = k_1 \sqrt{\varepsilon - \sin^2\theta_1}$$

A transmission curve for a slab having $\ell = 1/8"$ and $\varepsilon = 2.59$ is shown in Fig. 7 (Curve 4).

3e. Wire screens: In Fig. 6a, an H-mode propagates through a dielectric loaded with thin, conducting wires aligned parallel to the E-vector. Such obstacles present a shunt inductance, just what is required, according to Sec. 2, to reduce the effective dielectric constant.

The equivalent circuit, Fig. 6b, is a transmission line --characteristic impedance, Z, propagation constant K -- loaded periodically by shunt susceptances.

Instead of the infinite medium of Fig. 6a, we shall analyze the two cases shown in Figs. 6c and 6e, the equivalent circuits of which are shown in Figs. 6d and 6f respectively. Fig. 6c is obtained by slicing a section midway between the screens in Fig. 6a; Fig. 6e follows from Fig. 6a by excising a section that bisects the screens (this must be understood as bisecting the shunt admittances rather than an actual mechanical bisection -- that is, Fig. 6f, rather than Fig. 6e, describes the situation more accurately.)

We have computed the transmission through the slabs of Figs. 6c and 6e by reducing them to the homogeneous case shown in Figs. 5a, b. The necessary equations, derived in Sec. 4b, show that the propagation constant, κ_2, of the equivalent homogeneous slab, is the same in both cases; putting $B = \beta/Z = \beta Y$, in (4b-3),

$$\cos \kappa_2 \ell = \cos K\ell - \beta/2 \sin K\ell \tag{3e-1}$$

where K is the propagation constant of the unloaded line. The value of Z_2/Z_1, however, differs for each case. For Figs. 6c, d, since (4b-8) is appropriate,

$$\frac{Z_2}{Z_1} \sin \kappa_2 \ell = \frac{Z}{Z_1} \sin K\ell \left[1 - \beta/2 \tan k\ell/2\right] \tag{3e-2}$$

while, for Figs. 6e, f, since (4b-4) applies,

(3e-3) $$\frac{Z_2}{Z_1} \cdot \sin K_2 \ell = \frac{Z}{Z_1} \sin K\ell \ .$$

If the subscript "2" is dropped in (3b-1) and (3d-2), the resulting expressions correctly represent the values of K and Z/Z_1 to be used in the formulas above.

β may be obtained from the susceptances, given in the Waveguide Handbook[7], for inductive posts in free space. Two remarks are necessary. First, for thin wires, the series arms of the equivalent circuit may be neglected. Second, the influence of the dielectric--completely surrounding the wires in Fig. 6c, only partly in Fig. 6e--must be considered. This is discussed in Sec. 4d. The conclusion is that the absolute shunt admittance, jB (as distinct from the relative shunt admittance jB/Y), is unaffected, to the first order, by a change in ε. Thus, the values given for bare wires in the Waveguide Handbook, if reduced to absolute admittances, may be applied directly to Figs. 6c, e.

A theoretical formula is given in the Waveguide Handbook[7] for the shunt reactance X_a ($= -\frac{1}{B}$) of the wires. Taking only the first term of this expression*

(3e-4) $$\beta = \frac{B}{Y} = - \frac{2\pi}{Ka \ \ell n \ a/\pi d}$$

where d is the diameter of the wires and a is the spacing.

---

* This produces an error of $\lesssim 10\%$. The resulting accuracy is sufficient for the illustrative purposes in mind here.

These equations suffice to analyze the structures of Figs. 6c and 6e. The results, for transmission, P_t, phase shift, Δ, and the admittance of the equivalent homogeneous line, are given in Table I; transmission and phase shift curves are plotted in Fig. 7, with a plain dielectric slab plotted for comparison (Sec. 3d). The constants used, suggested by Worthington's work, are:

$$\lambda_1 = 1.26" \qquad \varepsilon = 2.59"$$
$$\ell = .125" \qquad d = .001"$$

These values are common to all the curves. For curve 1, Worthington's value, a = .266" was used. A calculation, based on the equivalent circuit, implied that a better match might be obtained for a = .280". This value was used for curve 1'. The low angle behavior, as expected, is improved, but curve 1' falls off more rapidly at large angles than curve 1. (For curves 1 and 1' the wires are imbedded in the center of the slab.)

Actually, this is not so bad as it seems, for, according to Table I, at angles $\sim 85^\circ$ and above, curve 1 is really beyond cut-off, while curve 1' is not. Thus, if the thickness were increased, 1 would drop rapidly while 1' would only oscillate.

Curve 2, where there is a set of wires on each side of the slab, assumes "a" adjusted so that the susceptance of each wire screen is 1/2 that of the screen of curve 1. Thus, curves 1 and 2 are related to each other as Figs. 6c and 6e.

Curve 3, with the same wire configuration as in curve 2, shows the effect of increasing "a" to .5", while curve 4 is the plain dielectric slab.

The flatness of these curves is quite surprising; their quantitative behavior seems quite close to Worthington's experimental results.

3f. Dissipation: In the previous discussion, the dielectrics were assumed lossless. If the dielectric constant has the real part ε' and the imaginary part ε'', the attenuation constant α, is[8]

(3f-1) $$\alpha = \frac{\varepsilon''}{2} \quad \frac{k_1^2}{K}$$

where, k_1 is the wave number in free space, and, for ε'' small, K may be computed assuming $\varepsilon'' = 0$. For plexiglass, at λ=3 cm., $\varepsilon' = 2.59$, $\varepsilon'' = .0067$. Using (3d-2) (dropping the subscript "2") in (3f-1),

(3f-2) $$\alpha = \varepsilon'' \frac{\pi}{\lambda_1\sqrt{\varepsilon' - \sin^2\theta_1}} = \frac{.0167 in^{-1}}{\sqrt{2.59 - \sin^2\theta_1}} \sim .01 in^{-1}$$

The loss in power in passing through a 1/8" slab is therefore of the order of 1/2%. This correction is more than the reflected power over most of the range of curves 1, 1', and 2 in Fig. 7.

However, while reflected power may cause serious trouble, because of interference effects, dissipated power,

since it is removed from the system, usually is not troublesome. In most applications, dissipation as small as that encountered here may be ignored.

3g. Junction effects: We return to Figs. 2a, b. As in Sec. 3a, we wish to compute the power, P_t, transmitted into region 2 when unit power is incident from region 1. In Sec. 3a, the calculation was simplified by the approximation $n^2 \sim 1$; now, we shall use the exact value of n^2.

We take: $\varepsilon = 2.59$; $a/\lambda_1 = .4$. This value of a/λ_1 is very close to the value appropriate to the $\theta_0 = 0$ curve of Sec. 3a.

Our procedure, based on the results of Sec. 4c, is as follows:

i) We first take $\varepsilon_2 = \varepsilon_1 = 1$. Then, the equivalent circuit is known[6]. That is, $n^2 = 1$, and formulas for d and d', as functions of θ_1, are available[6]. With $a/\lambda_1 = .4$,

$$(3g\text{-}1) \qquad \frac{\lambda_1}{\lambda_{g_2}} = \sqrt{1 - \left(\frac{\lambda_1}{2a}\right)^2} = -j.748$$

Thus, the parallel plates are beyond cut-off. However, the formulas[6] for d and d' may still be used; applied to this case, they result in the curves of Fig. 8.

ii) We now have d, d', and n(= 1). This representation is transformed, using the formulas of p. 120ff. of the Waveguide Handbook, to an equivalent T-network relative to the

reference plane coinciding with the boundary between regions 1 and 2. The equations of the Waveguide Handbook are slightly modified because, according to (3g-1), K_2 (and therefore Z_2) is purely imaginary. The relevant equations are obtained by the replacements $K_2 \longrightarrow -j\left|K_2\right|$; $Z_2 \longrightarrow j\left|Z_2\right|$ in the equations of the Waveguide Handbook,

$$a = \frac{Z_{11}}{jZ_1} = -\frac{\alpha\beta + \gamma}{\beta - \alpha\gamma} \quad ;$$

(3g-2)
$$c = \frac{Z_{22}}{jZ_2} = \frac{1 + \alpha\beta\gamma}{\beta - \alpha\gamma} \quad ;$$

$$b = \frac{Z_{11}\,Z_{22} - Z_{12}^2}{Z_1\,Z_2} = \frac{\alpha - \beta\gamma}{\beta - \alpha\gamma};$$

where:
$$\alpha = \tan K_1 d$$

$$K_1 = \frac{2\pi}{\lambda_1}\cos\theta_1$$

$$\beta = j\tanh\left|K_2 d'\right|$$

$$K_2 = \frac{2\pi}{\lambda_{g_2}}$$

$$\gamma = \frac{-Z_2}{Z_1} = \frac{-j\,K_1}{\left|K_2\right|} = -j\,\frac{\cos\theta_1}{\left|\frac{\lambda_1}{\lambda_{g_2}}\right|}$$

iii) Now let $\varepsilon_2 = \varepsilon$. Then, K_2, Z_2 become K_2', Z_2', where

$$\frac{\lambda_1}{\lambda'_{g_2}} = \sqrt{\varepsilon - \left(\frac{\lambda_1}{2a}\right)^2} = 1.02$$

(3g-3) $$\frac{Z_2}{Z_2'} = \frac{\kappa_2'}{\kappa_2} = \frac{\lambda_{g_2}}{\lambda'_{g_2}} = \frac{1.02}{-j.748} = j\,1.37$$

iv) Sec. 4c now states that, if $\varepsilon_2 = \varepsilon$, the absolute impedances, Z_{11}, Z_{12} and Z_{22}, computed from (3g-2), are unaffected, to the first order in $\varepsilon - 1$. Thus, changing ε_2 from 1 to ε results in a, b. c, $\rightarrow$ a', b', c', where:

(3g-4)
$$a' = a$$
$$c' = \frac{Z_2}{Z_2'}\, c$$
$$b' = \frac{Z_2}{Z_2'}\, b$$

v) Using (3g-4) and the formulas of p. 121 of the Waveguide Handbook, we finally compute

(3g-5)
$$n'^2 \frac{Z_2'}{Z_1} = -\gamma' = \frac{1 + a'^2 + b'^2 + c'^2}{2\,(b' + a'c')} \pm \sqrt{\left(\frac{1 + a'^2 + b'^2 + c'^2}{2\,(b' + a'c')}\right)^2 - 1}$$

The $\pm$ sign distinguishes reciprocal values of γ'. These are fully equivalent (see below).

This sequence of steps furnishes the exact transformer ratio, n'^2, to replace the approximation, $n'^2 \cong 1$, used in Sec. 3a. In terms of n' and γ', we then have, for the reflection coefficient (power):

$$(3g\text{-}6) \qquad |R|^2 = \left|\frac{Z_2' n'^2 - Z_1}{Z_2' n'^2 + Z_1}\right|^2 = \left|\frac{1 + \gamma'}{1 - \gamma'}\right|^2$$

This equation is clearly unchanged if $\gamma' \longrightarrow \frac{1}{\gamma'}$. Thus, for our purposes, the choice of sign in (3g-5) is immaterial.

We have plotted, in Fig. 9, the transmitted power P_t, computed for unit incident power. A curve has also been drawn for the case $n'^2 = 1$. For this calculation, taking $n'^2 = 1$ is equivalent to ignoring the junction effect, and, as expected, this curve closely reproduces the $\theta_o = 0$ curve of Sec. 3a. (Fig. 3).

The difference between the two curves of Fig. 9 is a measure of the importance of the junction effect in Fig. 2a. The curve that exhibits the junction effect shows that the performance is deteriorated by the junction effect. This may be corrected for by changing the spacing between plates, "a". The effect of changing "a" may be estimated by a perturbation calculation.

4. Appendices

4a. Transmission and reflection formulas: The (voltage) reflection coefficient, R, due to a load Z_2 on the end of a transmission line of characteristic impedance Z_1 (Fig. 10a) is:

$$(4a\text{-}1) \qquad R = \frac{V \text{ reflected}}{V \text{ incident}} = \frac{Z_2 - Z_1}{Z_2 + Z_1}$$

Z_2 may be due to an infinite line of characteristic impedance Z_2 connected to line 1 as in Fig. 10b. The (voltage) transmission coefficient, T, for this case, is given by

$$(4a\text{-}2) \qquad T = \frac{V \text{ transmitted}}{V \text{ incident}} = 1 + R = \frac{2Z_2}{Z_2 + Z_1}$$

The powers, incident (P_i), reflected (P_r), and transmitted (P_T), are:

$$P_i = Y_1 \left|V_i\right|^2 ;$$

$$(4a\text{-}3) \qquad P_r = Y_1 \left|V_r\right|^2 = Y_1 \left|R\right|^2 \left|V_i\right|^2$$

$$P_T = Y_2 \left|V_T\right|^2 = Y_2 \left|T\right|^2 \left|V_i\right|^2$$

where:

$$(4a\text{-}4) \qquad P_i = P_r + P_T$$

If $P_i = 1$, therefore,

$$(4a\text{-}5) \qquad P_T = 1 - \left|R\right|^2 = 1 - \left|\frac{Z_2/Z_1 - 1}{Z_2/Z_1 + 1}\right|^2$$

These formulas apply to the junction of two semi-infinite dielectrics, or lines. We also wish formulas that express the transmission through a dielectric slab (Fig. 11a). The equivalent circuit is shown in Fig. 11b. We shall compute the reflection, R, and the transmission, T, due to an incident (voltage) wave of unit amplitude.

Because of the symmetry of Fig. 11b, it is equivalent to the superposition of Figs. 11c and 11d. In Fig. 11c, the incident waves are symmetrical about the plane of symmetry; therefore, the reflected waves are also symmetrical. In Fig. 11d, incident waves (and hence reflected waves) are anti-symmetrical about the plane of symmetry.

In Fig. 11c, the voltage is symmetrical about the symmetry plane. Therefore, the current is anti-symmetrical about this plane; that is, the current is zero on the plane, and an open circuit may be placed on this plane. Thus, β_e may be computed from Fig. 11e.

Similarly, Fig. 11d is equivalent to Fig. 11f, in which a short circuit is placed on the symmetry plane.

We shall therefore compute β_e and β_o from Figs. 11e, and 11f, and then use:

(4a-6)
$$R = \beta_e + \beta_o$$
$$T = \beta_e - \beta_o$$

In, Fig. 11e, the reflection coefficient is $2\beta_e$, and the impedance presented to line 1 by line 2 is $-jZ_2 \cot \kappa_2 \ell/2$.

Therefore, from (4a-1),

$$2\beta_e = \frac{\oplus\, j Z_2 \cot\kappa_2 \ell/2 \quad \oplus\, Z_1}{-\, jZ_2 \cot\kappa_2 \ell/2 \quad + Z_1} \tag{4a-7}$$

Correspondingly, from Fig. 11f,

$$2\beta_o = \frac{jZ_2 \tan\kappa_2 \ell/2 \quad - Z_1}{jZ_2 \tan\kappa_2 \ell/2 \quad + Z_1} \tag{4a-8}$$

Thus, we finally find, putting $Z = Z_2/Z_1 = 1/Y$, and $\varphi = \kappa_2 \ell$:

$$R = \beta_e + \beta_o = \frac{j\left(\frac{Z-Y}{2}\right)\sin\varphi}{\cos\varphi + j\left(\frac{Z+Y}{2}\right)\sin\varphi} \tag{4a-9}$$

$$T = \beta_e - \beta_c = \frac{1}{\cos\varphi + 1/2\ j\ (Z+Y)\ \sin\varphi}$$

And,

$$|R|^2 = \frac{\left(\frac{Z-Y}{2}\right)^2 \sin^2\varphi}{1+\left(\frac{Z-Y}{2}\right)^2 \sin^2\varphi}$$

$$|T|^2 = \frac{1}{1+\left(\frac{Z-Y}{2}\right)^2 \sin^2\varphi} = 1 - |R|^2 \tag{4a-10}$$

For unit incident power, these expressions give the power reflected from, and transmitted by, the slab.

4b. Impedance and propagation constant of a loaded line:

In this Section, we wish to establish the equivalence between a uniform line (Fig. 12c) and a line, either loaded at each end with the shunt admittance $jB/2$ (Fig. 12a), or loaded at the center with the shunt admittance jB.

A uniform line, of characteristic admittance Y, propagation constant K, may be represented by the π network of Fig. 12d, the relations for which may be written in the following equivalent forms:

$$Y_{11} = -j\,Y \cot Kl; \qquad Y_{11} - Y_{12} = j\,Y \tan Kl/2$$

$$Y_{12} = -j\,Y \csc Kl; \qquad \frac{Y_{11}}{Y_{12}} = \cos Kl \tag{4b-1}$$

Fig. 12a is obtained from Fig. 12d by adding $j\,B/2$ to each end. This leaves Y_{12} unchanged, but $Y_{11} \rightarrow Y_{11} + j\,B/2$. Thus, if we prime the elements of the π network corresponding to Fig. 12a,

$$\cos K'l = \frac{Y'_{11}}{Y'_{12}} = \frac{Y_{11} + j\,B/2}{Y_{12}} = \cos Kl - \frac{B}{2Y} \sin Kl \tag{4b-3}$$

the new characteristic admittance is related to the old by:

$$\frac{Y'}{\sin K'l} = j\,Y'_{12} = j\,Y_{12} = \frac{Y}{\sin Kl} \tag{4b-4}$$

Thus, (4b-3) and (4b-4) express the connections between Fig. 12a and Fig. 12c.

To relate Fig. 12b to Fig. 12c, we replace Fig. 12b by its equivalent, Fig. 12e. If we temporarily ignore the admittances $-j\,B/2$ at each end of Fig. 12e, the remainder forms two sections each similar to Fig. 12a. We can therefore apply (4b-3) and (4b-4) to these sections. Calling the characteristic admittance and propagation constant of the equivalent uniform line Y_o and κ_o,

$$\cos \kappa_o \ell/2 = \cos \kappa\ell/2 - \frac{B}{2Y} \sin \kappa\ell/2 \tag{4b-5}$$

$$\frac{Y_o}{\sin \kappa_o \ell/2} = \frac{Y}{\sin \kappa\ell/2}$$

Now we must consider the admittances $-j\,B/2$, which shunt each end of this line. Again we have a situation as shown in Fig. 12a. Applying (4b-3) and (4b-4) to this situation, we find the equivalence between Figs. 12b and 12c to be given by (4b-5) and:

$$\cos \kappa'\ell = \cos \kappa_o\ell + \frac{B}{2Y_o} \sin \kappa_o\ell$$

(4b-6)

$$\frac{Y'}{\sin \kappa'\ell} = \frac{Y_o}{\sin \kappa_o\ell}$$

(4b-5) and (4b-6) reduce to:

$$\cos \kappa'\ell = \cos \kappa\ell - \frac{B}{2Y} \sin \kappa\ell \tag{4b-7}$$

$$(4b\text{-}8) \qquad \frac{Y'}{\sin k'\ell}\left[1 - \frac{B}{2Y}\tan k\ell/2\right] = -\frac{Y}{\sin k\ell}$$

Comparing (4b-7) and (4b-8) with (4b-3) and (4b-4), we see that although the propagation constants are the same for Figs. 12a and 12b, the characteristic admittances are different.

4c. Interface admittances: In Section 3e, the problem of computing the equivalent circuit of Fig. 6e arose. Here, the difficulty lay in the fact that although a result was available (in the Waveguide Handbook) for the case where the obstacle was surrounded by a uniform medium, we required the solution of the problem where each half of the obstacle was immersed in a different medium. We wish to consider such problems here, limiting ourselves, however, to those cases where the equivalent circuit is a simple shunt element.

For H-mode problems, our point of departure will be the variational expression for the absolute value (as distinct from the relative value) of the shunt reactance, X:

$$(4c\text{-}1) \qquad -iX\left|I^{(1)} + I^{(2)}\right|^2 = \sum_{\text{Higher Modes}}\left\{Z_n^{(1)}\left|I_n^{(1)}\right|^2 + Z_n^{(2)}\left|I_n^{(2)}\right|^2\right\}$$

Here, quantities belonging to the regions on each side of the obstacle are identified by superscripts 1 and 2. The subscripts identify the mode numbers; the dominant mode does not carry a subscript. The higher mode characteristic impedances are (say

for line "1"):

$$(4c\text{-}2) \qquad Z_n^{(1)} = \frac{\omega \mu_1}{K_n} = \frac{\omega \mu_1}{\sqrt{\omega^2 \mu_1 \varepsilon_1 - k c_n^2}}$$

but under most conditions the K_n's are approximately equal to their "static" values and the Z_n's may be replaced by:

$$(4c\text{-}3) \qquad Z_{ns}^{(1)} = \frac{-i\omega\mu_1}{k c_n}$$

In this limit, ε_1 (or ε_2) does not appear explicitly in (4c-1). Its only influence is indirect, i.e., by changing the value of the exact field appropriate to the problem.

However, the variational principle automatically minimizes the effect of changes of the field. Hence, the value of X is unchanged, to the first order, by changing ε_2 or ε_1, from unity; i.e., changing ε_1 or ε_2 produces a second order change in the absolute impedance that represents the obstacle.

For E-modes the previous equations are replaced by:

$$(4c\text{-}1') \qquad -iB\,|V|^2 = \sum_{\substack{\text{Higher} \\ \text{Modes}}} \left\{ Y_n^{(1)} \left| V_n^{(1)} \right|^2 + Y_n^{(2)} \left| V_n^{(2)} \right|^2 \right\}$$

$$(4c\text{-}2') \qquad Y_n^{(1)} = \frac{w \varepsilon_1}{K_n} = \frac{\omega \varepsilon_1}{\sqrt{\omega^2 \mu_1 \varepsilon_1 - k^2 c_n}}$$

$$(4c\text{-}3') \qquad Y_{ns}^{(1)} = -i \frac{\omega \varepsilon_1}{k c_n}$$

Here, the variational principle for the absolute susceptance $|B|$ becomes, using (4c-3'),

$$(4c\text{-}4) \qquad B|V|^2 = \sum_{\substack{\text{Higher}\\ \text{Modes}}} \left\{ \frac{\omega \varepsilon_1}{k_{c_n}^{(1)}} \left| V_n^{(1)} \right|^2 + \frac{\omega \varepsilon_2}{k_{c_n}^{(2)}} \left| V_n^{(2)} \right|^2 \right\}$$

and there is a first order dependence on ε_1 and ε_2. Clearly, the effect of changing ε_1 or ε_2 from unity to another value depends on the relative strengths of the higher mode fields $V_n^{(1)}$ and $V_n^{(2)}$. If the field is concentrated, so that the coefficients $V_n^{(2)}$ are $\ll V_n^{(1)}$, the situation can arise where changing ε_1 has an appreciable effect while changing ε_2 does not.

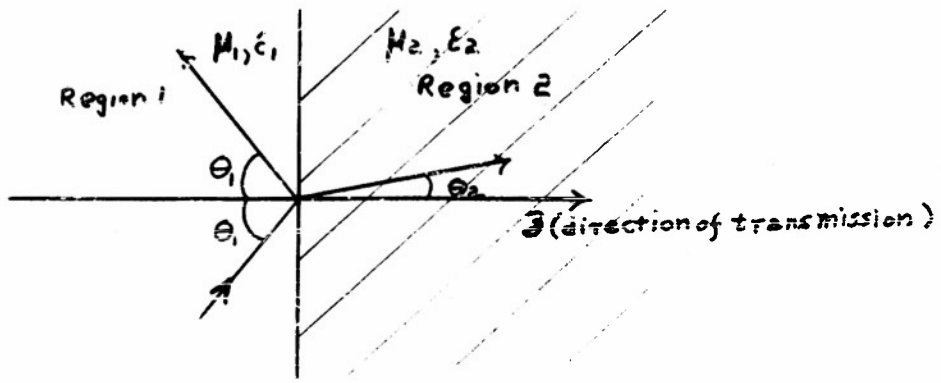

$k_i = \omega\sqrt{\mu_i \epsilon_i} = 2\pi/\lambda_i$; $\kappa_i^2 = k_i^2 - k_{ci}^2$; $\eta_i = \sqrt{\mu_i/\epsilon_i} = 1/n_i$

where $k_{ci} = k_i \sin\theta_i$ $\quad (i = 1, 2)$

Snell's Law ; $k_{c1} = k_{c2}$

FIG. 1a

E-modes

Characteristic admittance

$Y' = \eta k/\kappa = \omega\epsilon/\kappa = 1/Z'$

H-modes

Characteristic Impedance

$Z'' = \eta k/\kappa = \omega\mu/\kappa = 1/Y''$

Series Impedance / unit length

$Z_s' = j\kappa Z' = j\kappa^2/\omega\epsilon = j\omega\mu - jk_c^2/\omega\epsilon$

$Z_s'' = j\kappa Z'' = j\omega\mu$

Shunt admittance / unit length

$Y_s' = j\kappa Y' = j\omega\epsilon$

$Y_s'' = j\kappa Y'' = j\kappa^2/\omega\kappa = j\omega\epsilon - jk_c^2/\omega\mu$

as $\delta x \to 0$, the equivalent circuit of a length δx is:

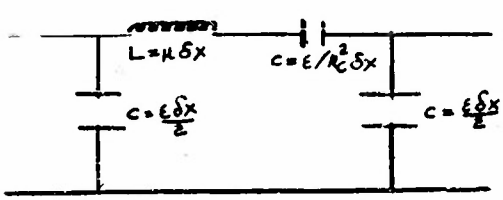

FIG. 1b

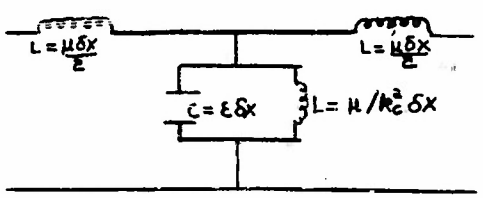

FIG. 1c

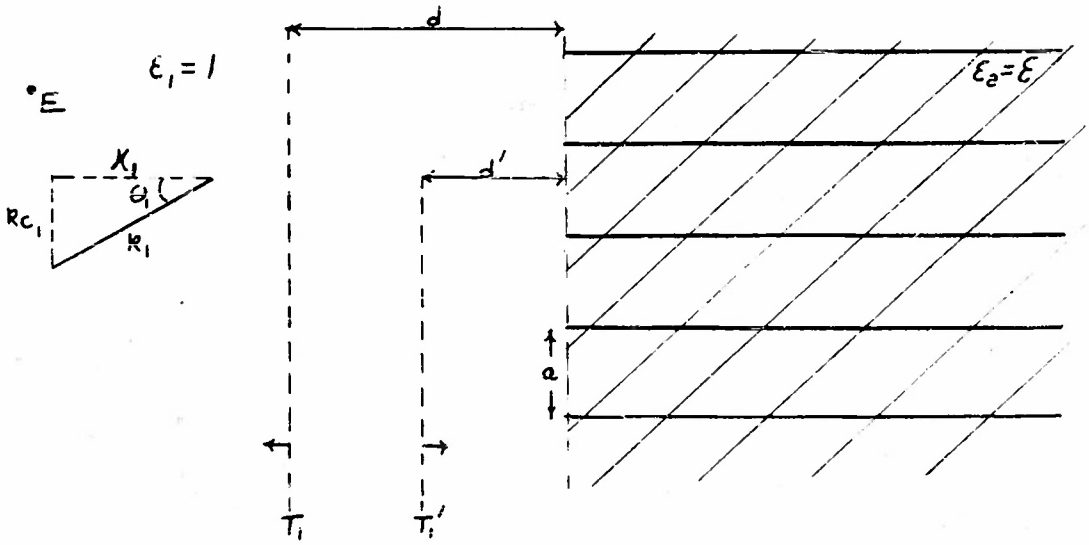

FIG. 2a

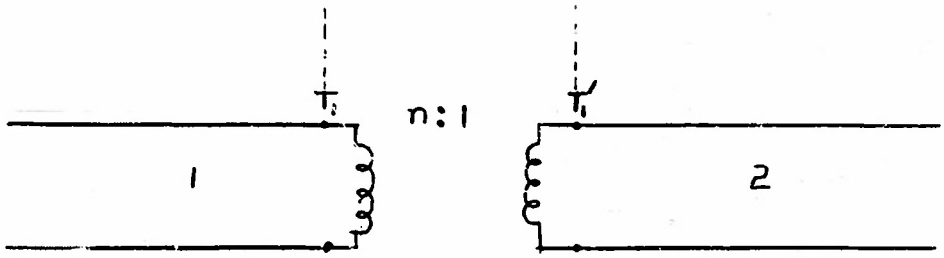

$$\frac{Z_2}{Z_1} = \frac{K_1}{K_2} = \frac{K_1 \cos\theta_i}{K_2}$$

FIG. 2b

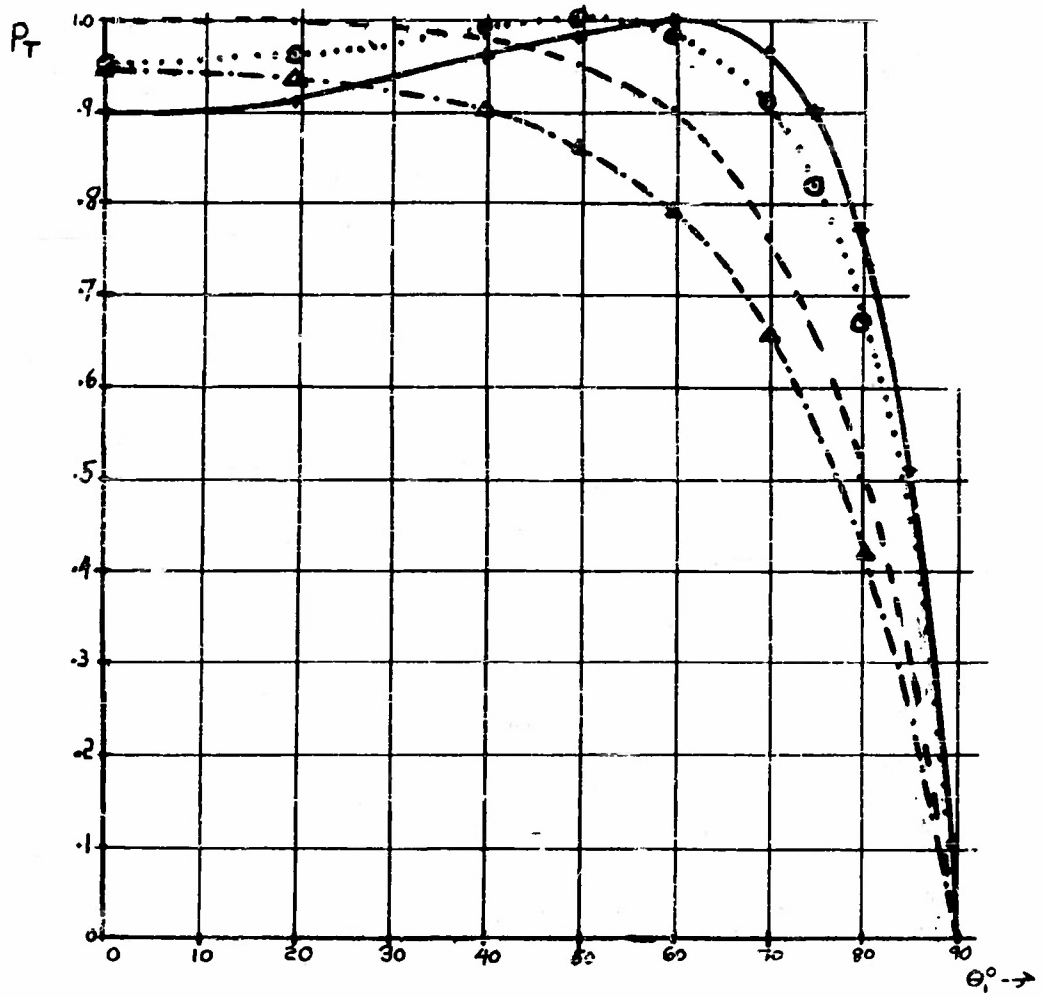

$\theta_0^\circ = 0^\circ$: · – – – – –

$\theta_0^\circ = 50^\circ$: ⊙ · · · · · · ·

$\theta_0^\circ = 60^\circ$: + ———

Semi infinite dielectric slab ; △—·—·—·—

FIG. 3

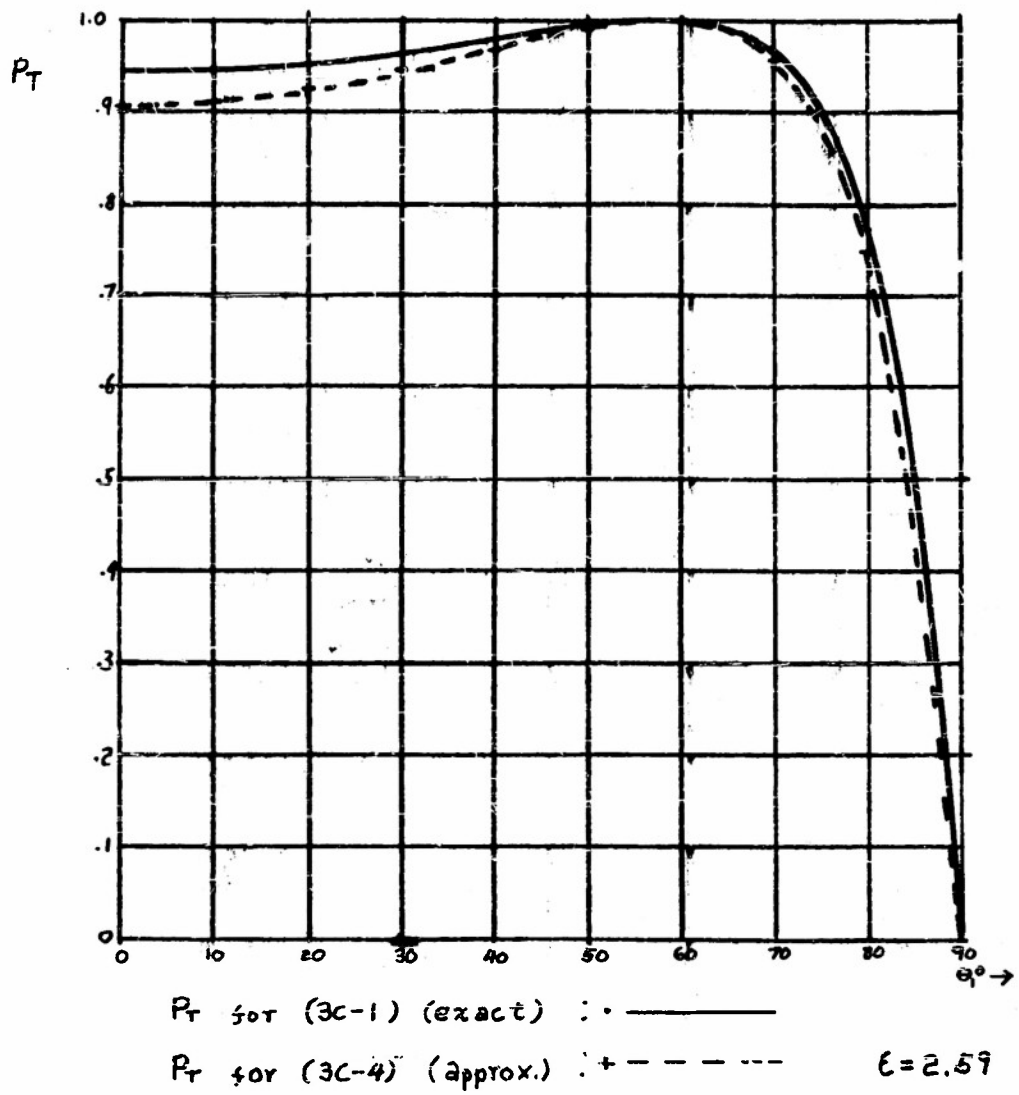
P_T
1.0
.9
.8
.7
.6
.5
.4
.3
.2
.1
0
0
10
20
30
40
50
60
70
80
90
θ° →
P_T for (3C-1) (exact) : • ————
P_T for (3C-4) (approx.) : + — — — ---
ε = 2.59

FIG. 4

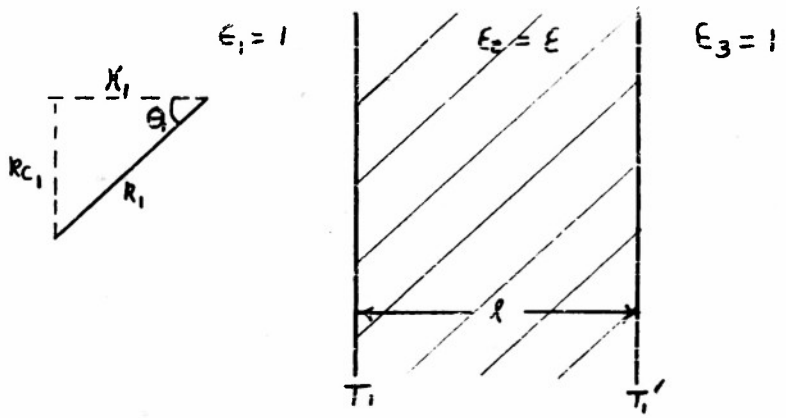

$$K_2 = K_1\sqrt{\epsilon} \; ; \quad K_3 = K_1 \; ; \quad K_{C_1} = K_{C_2} = K_{C_3}$$

FIG. 5a

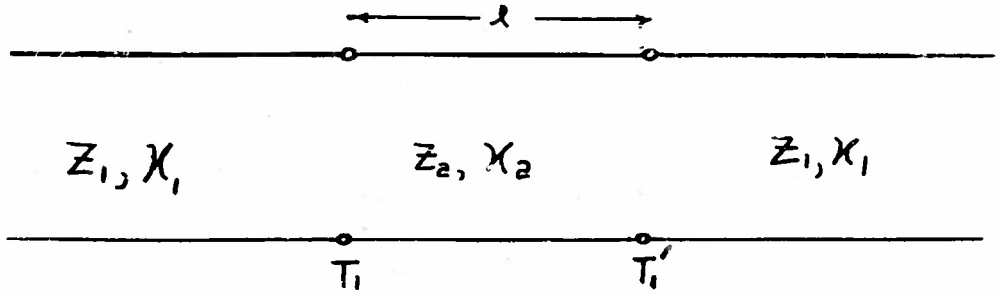

FIG. 5b

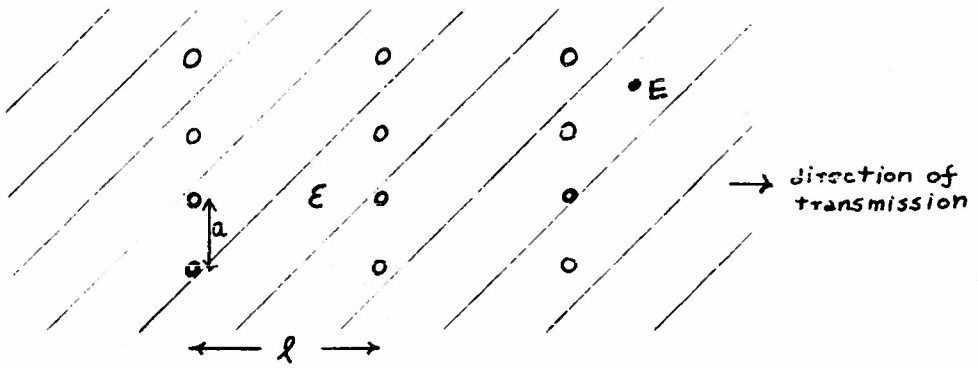

FIG. 6a

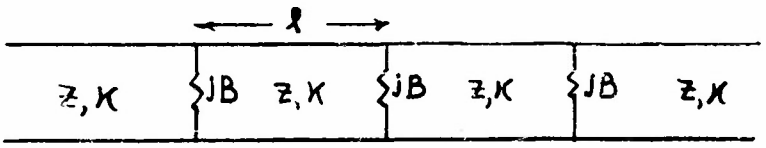

FIG. 6b

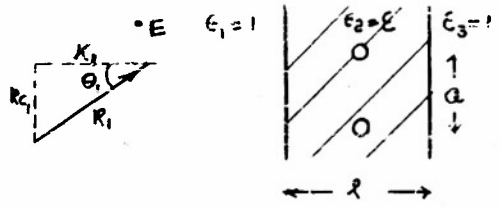

FIG. 6c

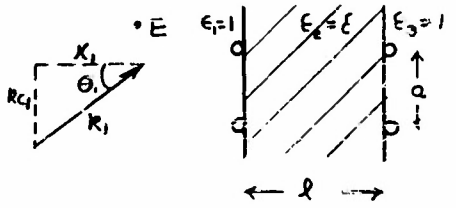

FIG. 6e

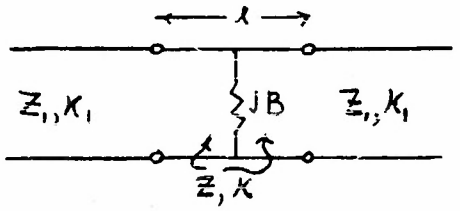

FIG. 6d

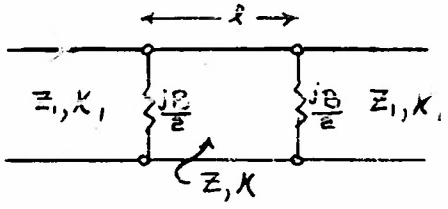

FIG. 6f

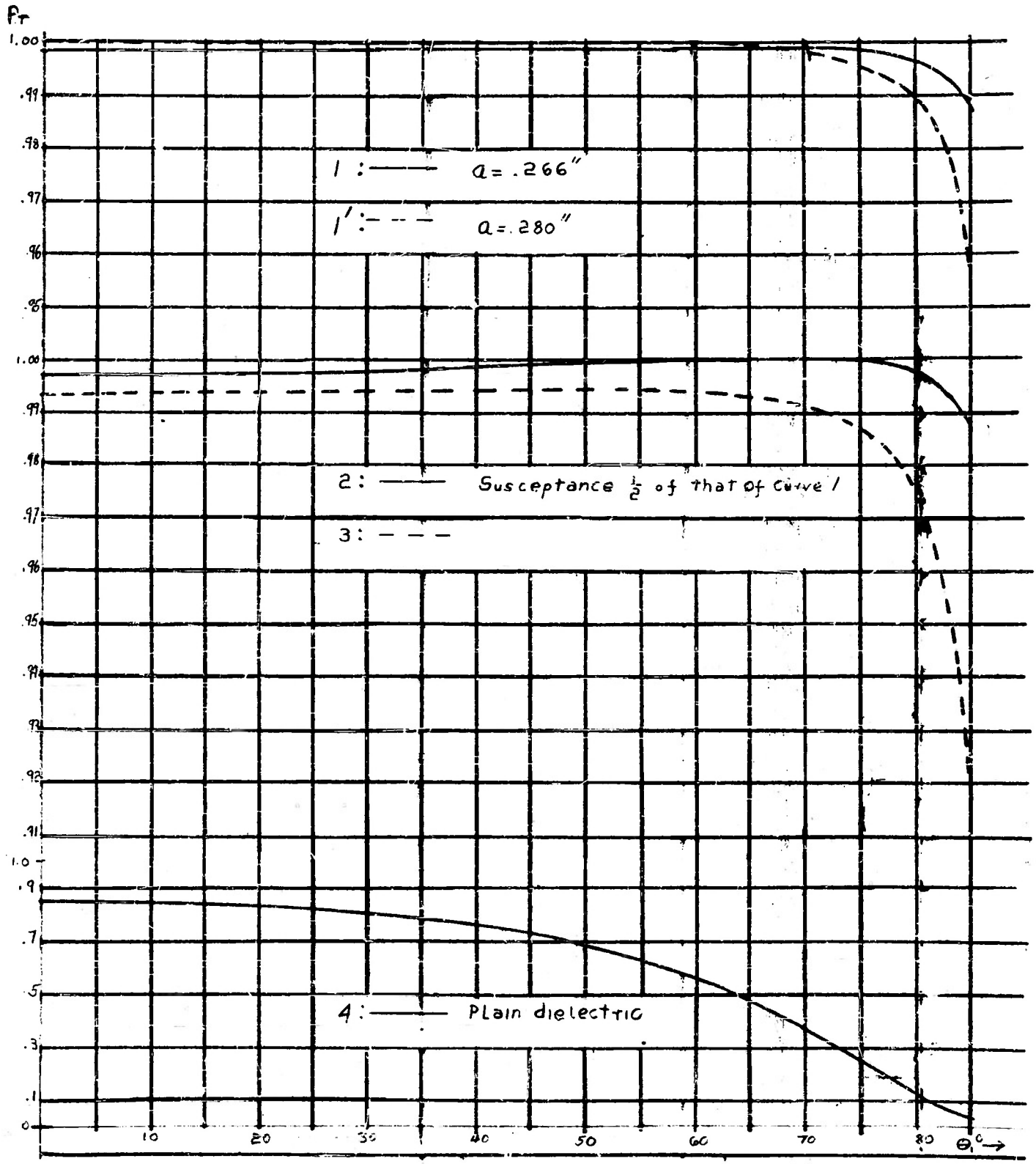
P_T
1.00
.99
.98
.97
.96
.95
1.00
.99
.98
.97
.96
.95
.91
.92
.91
1.0
.9
.7
.5
.3
.1
0
10
20
30
40
50
60
70
80
θ,°
1 : —— a = .266"
1' : - - - a = .280"
2 : —— Susceptance ½ of that of curve 1
3 : - - -
4 : —— Plain dielectric

FIG. 7a

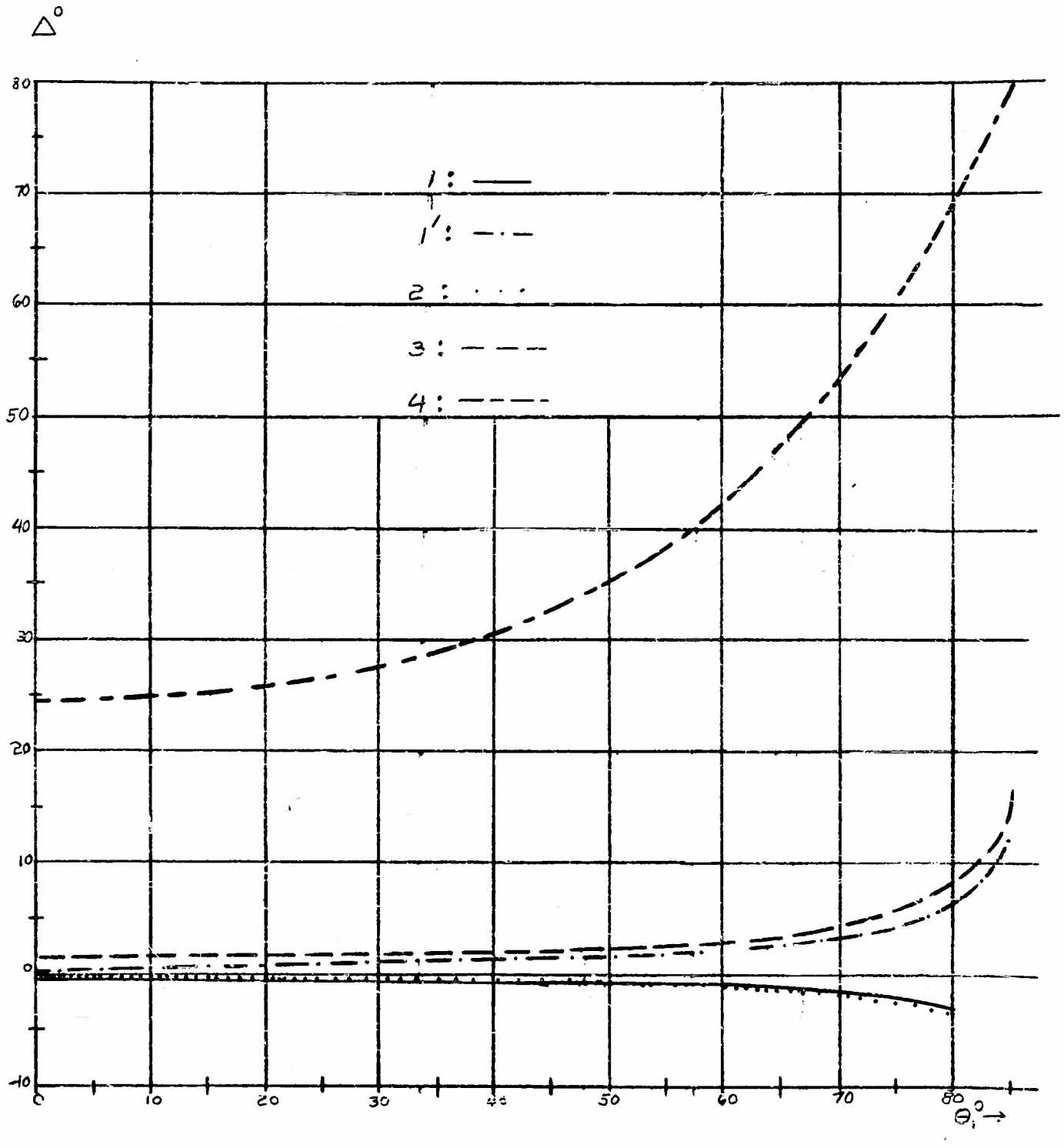

Fig. 7b

TABLE I

	1			1'		
$\theta_1°$	P_T	$\Delta°$	Y_2/Y_1	P_T	$\Delta°$	Y_2/Y_1
0	.99831	-.434	.9313	.99983	.167	.97843
10	.99834	-.450	.9309			
20	.99841	-.484	.9295			
30	.99853	-.534	.9270	.99996	1.300	.98816
40	.99865	-.616	.9216			
50	.99878	-.767	.9114			
60	.99882	-1.000	.8877	.99956	2.167	1.06319
70	.99858	-1.484	.8426	.99813	3.150	1.17899
80	.99675	-2.934	.0332	.98978	6.150	1.67166
85	.9880	*	-j1.6442 *	.95749	12.067	2.89845

	2			3			4	
$\theta_1°$	P_T	$\Delta°$	Y_2/Y_1	P_T	$\Delta°$	Y_2/Y_1	P_T	$\Delta°$
0	.99694	-.383	1.10059	.993	1.534	1.1481	.8521	24.534
10	.99706	-.400	1.09999	.993	1.633	1.1519	.8477	25.192
20	.99742	-.434	1.09776	.993	1.733	1.1562	.8335	25.918
30	.99794	-.500	1.09394	.993	1.850	1.1635	.8068	27.742
40	.99861	-.616	1.08664	.994	2.000	1.1753	.7616	30.700
50	.99928	-.800	1.07357	.994	2.350	1.2022	.6871	35.250
60	.99984	-1.100	1.04478	.994	2.967	1.2595	.5651	42.225
70	.99994	-1.684	.95783	.991	4.333	1.4167	.3739	52.908
80	.99765	-3.416	.03900	.975	8.450	2.0661	.1320	69.033
85	.98678	*	-j1.93263*	.917	16.400	3.6433	.0368	79.108

*Beyond Cutoff

$$\Delta = \varphi - K\ell \; ; \quad \tan\varphi = \frac{1 + (Y_2/Y_1)^2 \tan K_2 \ell}{2(Y_2/Y_1)}$$

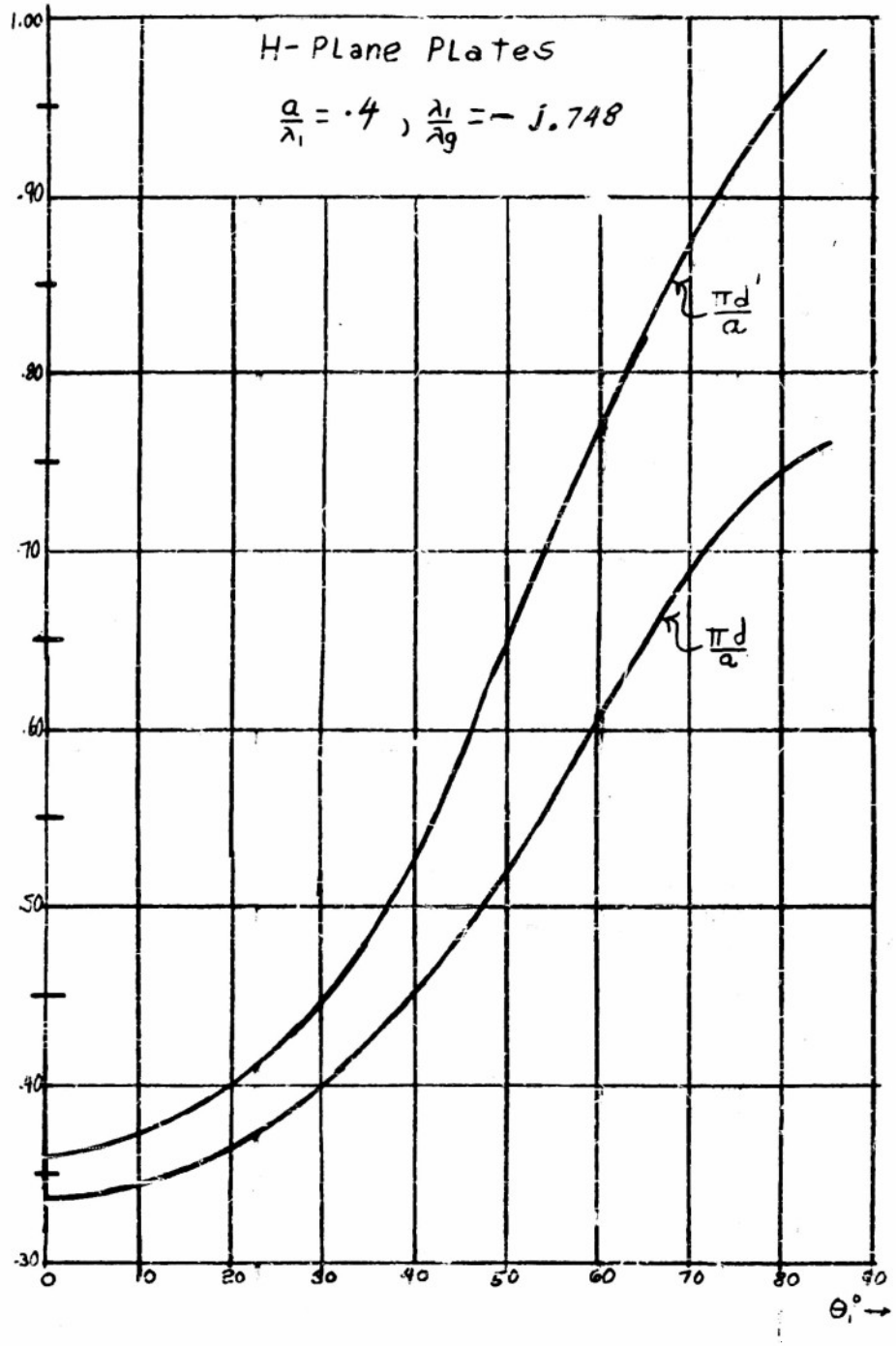
H- Plane Plates
$\frac{a}{\lambda_1} = .4$, $\frac{\lambda_1}{\lambda_g} = -j.748$
1.00
.90
.80
.70
.60
.50
.40
-.30
0
10
20
30
40
50
60
70
80
90
$\theta_1^\circ \rightarrow$
$\frac{\pi d'}{a}$
$\frac{\pi d}{a}$

FIG. 8

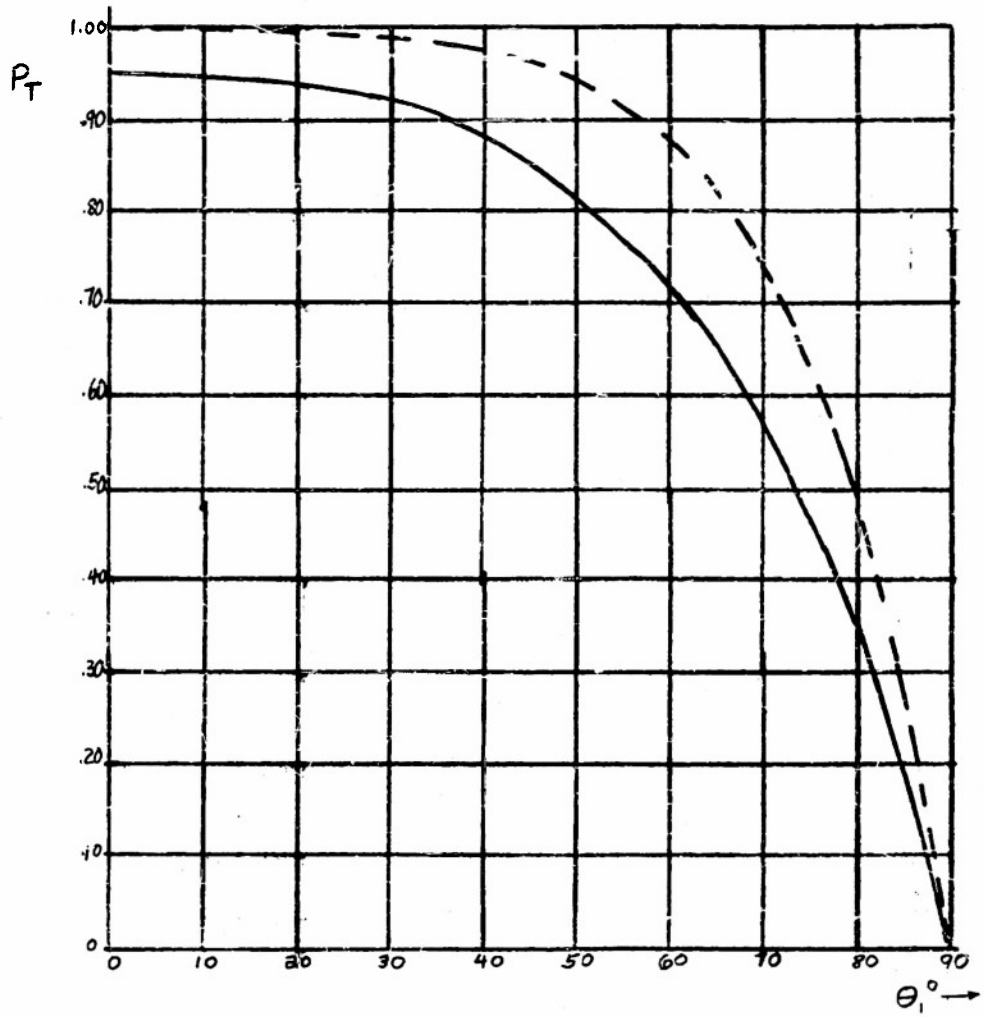

No junction effect ($n^2=1$) : — — —

With junction effect : ————

FIG. 9

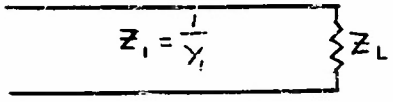

FIG. 10a

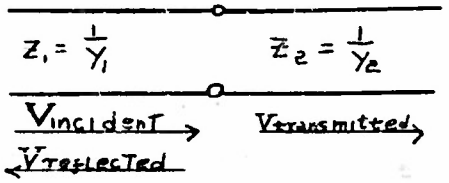

FIG. 10b

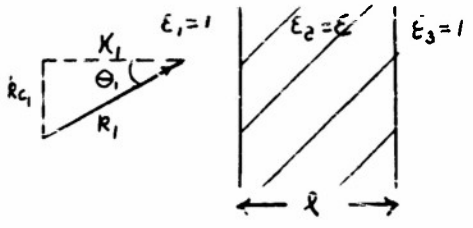

FIG. 11a

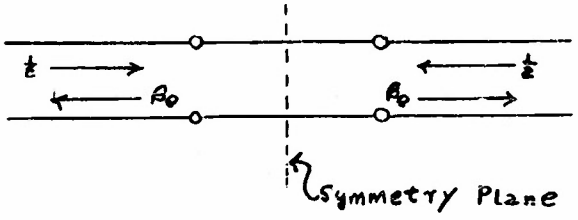

FIG. 11c

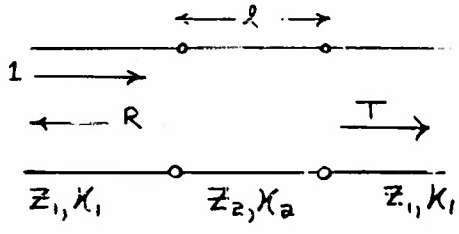

FIG. 11b

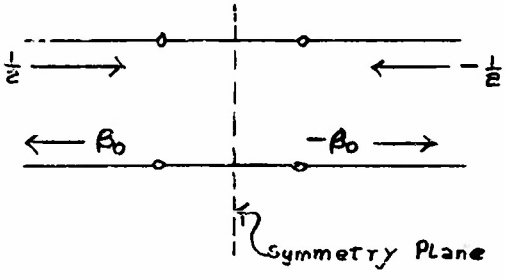

FIG. 11d

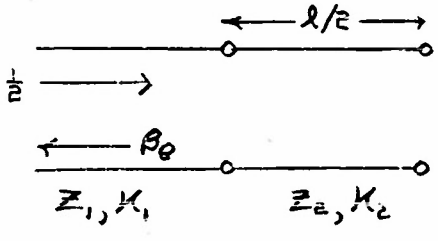

FIG. 11e

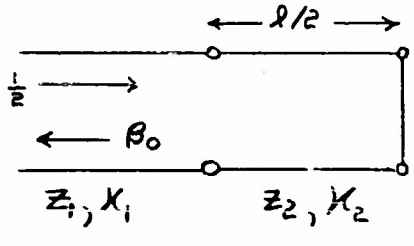

FIG. 11f

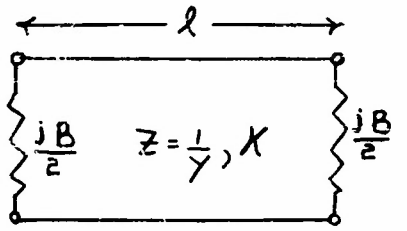

FIG. 12a

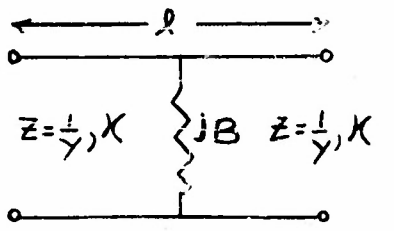

FIG. 12b

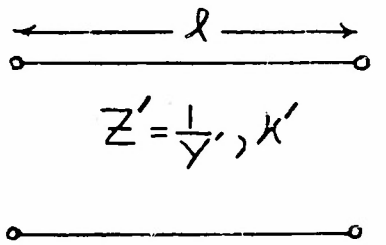

FIG. 12c

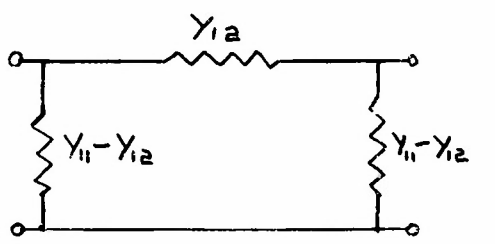

FIG. 12d

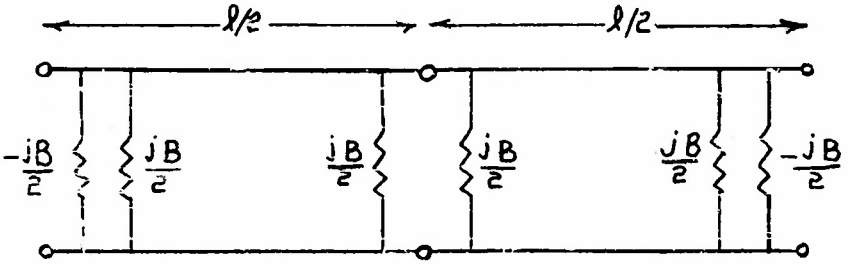

FIG. 12e

FOOT-NOTES

1. Final Report, Princeton University Radome Study, Contract No. N60nr-27023 (1 March 1952). (Secret)
2. Bjorksten Research Laboratories, Madison, Wisconsin.
3. Marcuvitz, N., Waveguide Handbook, Vol. 10, p. 84ff, Radiation Laboratory Series, McGraw-Hill (1951).
4. We use the notation of the Waveguide Handbook, Chapter 1
5. Waveguide Handbook, p. 117ff.
6. Waveguide Handbook, p. 290; compare p. 172.
7. Waveguide Handbook, p. 286.
8. Waveguide Handbook, p. 18.